ELSEVIER

Contents lists available at ScienceDirect

# **Food Chemistry**

journal homepage: www.elsevier.com/locate/foodchem





# Utilisation of yeast biomass to stabilise oil-in-water emulsions<sup>★</sup>

Sowmya Narsipur <sup>a,b</sup>, Qifei He <sup>b</sup>, Ben Kew <sup>b,c</sup>, Célia Ferreira <sup>b</sup>, Anwesha Sarkar <sup>b,c,\*</sup>

- <sup>a</sup> School of Chemical and Process Engineering, University of Leeds, Leeds LS2 9JT, UK
- <sup>b</sup> Food Colloids and Processing Group, School of Food Science and Nutrition, University of Leeds, Leeds LS2 9JT, UK
- c National Alternative Protein Innovation Centre (NAPIC), UK

## ARTICLE INFO

Keywords: Alternative protein Sustainability Emulsifier Pickering emulsion

#### ABSTRACT

This study aimed to understand the role of yeast biomass in stabilising oil-in-water emulsions. Three food-grade yeast strains (Saccharomyces cerevisiae (SC) including two non-conventional strains of yeast (NC1 and NC2)) were cultured using batch fermentation to obtain their biomass (size range 1–10  $\mu m$ ) and were used to stabilise 5–20 wt% oil-in-water emulsions. The oil-in-water emulsions, stabilised by biomass demonstrated varying stabilisation capacities, with SC preventing droplet coalescence for four weeks with mean droplet size (d [4,3])  $\sim 12~\mu m$  whilst emulsions made using NC1 or NC2 showed rapid coalescence within a week. Washing of the SC biomass resulted in emulsion destabilisation and increase of interfacial tension of the n-tetradecane/water interface, associated with removal of loosely-bound proteins from the cells. In summary, our findings pinpoints the potential contribution from other surface-active agents such as surface/ secreted proteins in the SC biomass stabilising the emulsions droplets rather than a true Pickering stabilisation.

## 1. Introduction

Today, plant proteins such as soy, pea, chickpea, oat and lupin mainly dominate the alternative protein landscape (Ma et al., 2022; McLauchlan et al., 2024) as a result of research and industrial efforts to reduce animal protein-associated carbon footprint. However, microbial cells from fungi, yeast, bacteria and algae are gradually gaining increased attention in literature, in the form of biomass but also in precision fermentation to produce alternative sustainable sources of protein using microbial cells as cell factories. A well-known example of biomass fermented protein is Quorn™, which is a commercially available meat analogue, made from the filamentous fungi *Fusarium venenatum* combined with animal or plant proteins (Okeudo-Cogan et al., 2023; Okeudo-Cogan et al., 2024; Okeudo-Cogan et al., 2025; Pérez-Torrado et al., 2015). Besides meat analogues, there is an increased attention to test the efficacy of microbial cells to stabilise food emulsions (Dorobantu et al., 2004; Jiang et al., 2019).

Within the fungal proteins, there is a burgeoning interest in biomass fermentation of yeasts (Martin & Chan, 2024; Wani et al., 2023) in recent years with a renewed focus to use yeast as source of functional alternative protein. Although commercially available *Saccharomyces cerevisiae* (SC) or dehydrated form of Baker's yeast have been applied in

bakery and beverage applications for centuries (Parapouli et al., 2020), there is limited study so far on the ability of yeast cells to emulsify oil droplets (Narsipur et al., 2024). Among such yeast cell-based emulsion studies, few have suggested that yeast cells have an ability to stabilise oil-in-water emulsions *via* a Pickering stabilisation mechanism (Firoozmand & Rousseau, 2016; Furtado et al., 2015; Meirelles et al., 2018; Moreira et al., 2016).

Typically, such dehydrated Baker's yeast has been redispersed in aqueous phase to stabilise Pickering emulsions, where yeast cells adsorb to droplet surfaces, identified as the primary mechanism behind emulsion stabilisation. In other words, once the yeast cell has been attached to an oil-water interface at a finite contact angle (closer to 90°), it can be considered to be irreversibly adsorbed as large quantity of desorption energy is required to remove the particle from the interface (Sarkar & Dickinson, 2020). Noteworthy, commercially available dried yeast for brewing or baking applications contain two ingredients: the baker's yeast (e.g. Saccharomyces cerevisiae) and an emulsifier (usually sorbitan monostearate, often listed as E491 (Mortensen et al., 2017). One might question the importance of co-emulsifier in the stabilisation mechanism, besides the Pickering stabilisation reported previously.

In general, yeast cell is enclosed by a rigid cell wall composed of a complex network of polysaccharides and proteins, primarily beta-

 $<sup>^{\</sup>star}$  This article is part of a Special issue entitled: '3rd NIZO Plant Protein' published in Food Chemistry.

<sup>\*</sup> Corresponding author at: Food Colloids and Processing Group, School of Food Science and Nutrition, University of Leeds, Leeds LS2 9JT, UK *E-mail address*: A.Sarkar@leeds.ac.uk (A. Sarkar).

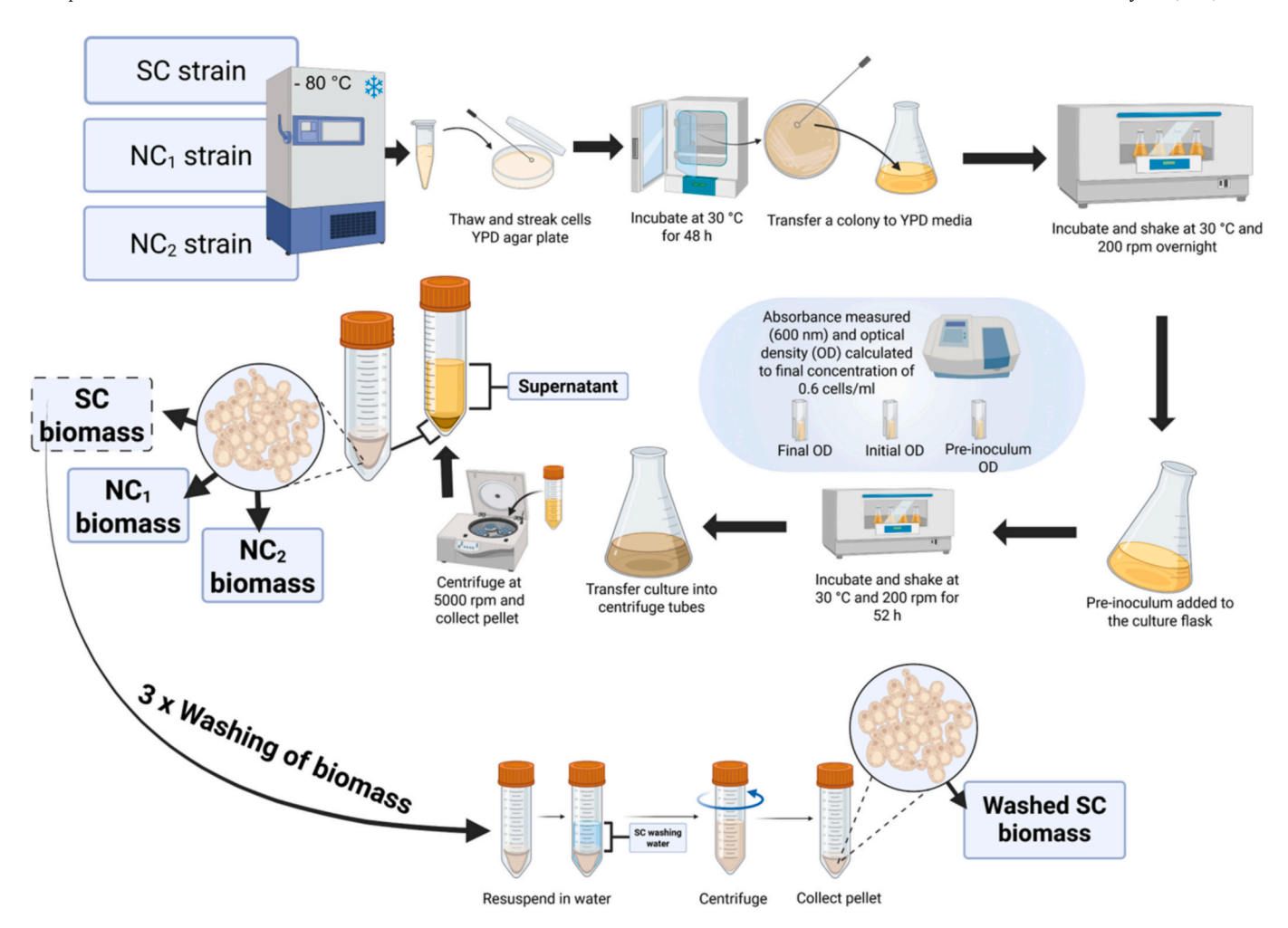


Fig. 1. Schematic illustration of experimental method for preparation of yeast biomasses (SC,  $NC_1$  and  $NC_2$ ). In SC, both unwashed and washed biomass have been prepared.

glucans, chitin, and mannoproteins (Lipke & Ovalle, 1998), the latter is predominantly located on the outer surface. Mannoproteins has been often cited in literature for their ability to stabilise emulsions besides other cell wall proteins and other biosurfactants (Neto & Silva, 2026; Saito et al., 2025). Nevertheless, there is ongoing debate on key mechanism of stabilisation of emulsions by the surface-active mannoproteins forming a molecularly-adsorbed interfacial layer *versus* a Pickering-type stabilisation by the intact yeast cells themselves (Cameron et al., 1988; Nerome et al., 2023; Qiao et al., 2022; Silva Araújo et al., 2014). For instance, Onishi et al. (2021) identified SC-derived mannoproteins being responsible for emulsifiying oil-in-water (O/W) emulsions. On the other hand, Nerome et al. (2020) suggested that high molecular weight materials released from yeast cells contribute to emulsion stabilisation.

Overall, it remains to be investigated whether the biomass of yeast has such true Pickering-like behaviour at the oil-water interface, similar to rehydrated yeast particles, as reported in literature. It remains unclear whether washed yeast biomass behave similarly to those of unwashed biomass, pinpointing any role that the cell surface proteins may have in stabilising droplet. Furthermore, the mechanisms of emulsion stabilisation may vary between yeast strains, particularly when exploring nonconventional yeasts. Hence, the aim of this study was to understand the functional properties of yeast biomass as stabilisers of oil-water interfaces using conventional as well as non-conventional yeasts. Our hypothesis was yeast biomass irrespective of the yeast strains will be able to stabilise emulsions *via* a Pickering-type stabilisation. In order to examine the hypothesis, we generated biomass of three types of yeast strains using a batch-fermentation approach in the laboratory and

employed a suite of characterisation techniques ranging from light scattering, microscopy across length scales (scanning electron microscopy, confocal laser scanning microscopy), rheology, interfacial tension measurements and stability studies. We also carried out washing of the cells and characterising the composition of the wash water to understand whether the cells themselves contribute to stabilisation of droplets or the proteins that are either located at the surface or secreted *via* disruption of cells during homogenisation contribute to the stabilisation of droplets.

## 2. Materials and methods

# 2.1. Materials and chemicals

Three yeast strains, *i.e.* Saccharomyces cerevisiae (SC), and non-conventional yeast strains (NC<sub>1</sub> and NC<sub>2</sub>) were provided by Cândida Lucas from School of Biology of Minho University, Portugal. Yeast Peptone Dextrose (YPD) broth powder was purchased from MP Biomedicals (Santa Ana, USA) and the agar powder was purchased from Merck, Germany. Sunflower oil was purchased from a local supermarket (Sainsbury's, UK) and the sodium azide was purchased from Sigma-Aldrich (Dorset, UK). Pierce BCA Protein Assay Kit was used from Thermo Scientific (Oxford, UK) while the gels, reagents and apparatus used for sodium dodecyl sulphate polyacrylamide gel electrophoresis (SDS-PAGE) were from the Invitrogen NuPAGE line by Thermo Scientific (Oxford, UK). All other chemicals were of analytical grade and were purchased from Sigma-Aldrich (Dorset, UK) unless otherwise specified.

Ultrapure water (resistivity 18.2 M $\Omega$ /cm) from a Millipore Milli-Q system (Millipore Corp., Bedford, MA, USA) was used as a solvent to make the buffer.

#### 2.2. Biomass fermentation

Three types of yeast strains (SC,  $NC_1$  and  $NC_2$ ) were cultured in a single-cell stage using a small-scale, batch fermentation process on a YPD media with air-to-liquid ratio of 2.5:1  $\nu/\nu$  for 54 h until their late stationary phase was achieved as illustrated in Fig. 1 (Held, 2010). Culture flasks were placed in an incubator shaker set at 30 °C with a constant shaking speed of 200 rpm for 54 h. The shaking of the flasks allowed for even distribution of free oxygen within the culture media and among the yeast cells. The pH of the culture media at the start of fermentation was pH 6.08, while at the end of the fermentation was pH 6.49. The concentration of cells was determined using optical density (OD) at initial inoculation and post 54 h fermentation with absorbance measured at 600 nm. After reaching a high cell population (OD<sub>600 nm</sub> of  $\sim$ 14), a biomass pellet was obtained by centrifuging the yeast cultures at 4696 g for 5 min. The biomass fermentation is illustrated schematically in Fig. 1.

#### 2.3. Interfacial tension

Exactly, 0.1 vol% of SC, NC<sub>1</sub> and NC<sub>2</sub> biomass was dispersed in 20 mM phosphate buffer at pH 7.0 and interfacial tension (IFT) was measured using the OCA 25 (Dataphysics Instruments, Germany) to capture the image of the drop and the Young-Laplace equation was used to calculate the interfacial tension (Berry et al., 2015; Inaba & Sato, 1996). A 1.65 mm straight needle (SNP 165/119) was used to dispense the sample into a cuvette containing *n*-tetradecane, which served as the oil phase. n-Tetradecane was chosen due to its widespread use as a standard in the literature (Akgonullu et al., 2024). The measurements were performed at 22 °C, and the interfacial tension was measured at every one-second interval for up to 1200 s. The Young-Laplace equation was fitted to the extracted shape of the drop obtained using dpiMAX software. Control samples i.e. n-tetradecane-buffer interface was also measured without any added biomass. Results are presented as means and standard deviations, based on at least triplicate measurements conducted on three independent samples ( $n = 3 \times 3$ ).

# 2.4. Scanning electron microscopy (SEM)

Morphological characteristics of the biomass was assessed using scanning electron microscopy (SEM). Briefly, the biomass sample was placed on an SEM stub and allowed to dry using hot air until the water was completely evaporated. Biomass was then coated with carbon prior to imaging on a bench-top Hitachi TM3030 Scanning Electron Microscope (SEM) at a voltage range of 15 to 30 kV. Images were analysed using ImageJ software (version 1.48r, National Institute of Health, Bethesda, USA) to determine the maximum dimension of the biomass, calculated using at least 100 cells in multiple images. The sizes were calculated using FIJI (ImageJ software).

# 2.5. Emulsion preparation

SC,  $NC_1$  and  $NC_2$  yeast strains (1 vol% cell) were dispersed in 20 mM phosphate buffer at pH 7.0. Oil-in-water emulsions (5–20 wt% oil) were mixed with the biomass dispersions with a high-speed homogeniser (Ultra Turrax T25, IKA-Werke GmbH & Co., Germany) set at 7500 rpm speed for 2 min. This dispersion was then passed through the high-pressure Leeds Jet Homogeniser (School of Food Science and Nutrition, University of Leeds, UK) with an opening of 3.5 mm at 300 bar pressure to obtain the final emulsion and they were stored refrigerated at 5 °C until subsequent analyses were performed.

#### 2.6. Washing of biomass and emulsion preparation

A small aliquot of culture SC biomass were washed with sterile MilliQ water to remove compounds from the growth media or any surface proteins that were attached externally to the cells that would influence the emulsification process. This was done to understand the interfacial effect of washed *versus* unwashed biomass. Washed SC biomass was prepared by resuspending the pellet in Milli-Q water, followed by a centrifugation step. The washing and centrifugation steps were repeated three times to remove any surface proteins. Then these washed cells (Fig. 1) were used to prepare oil-in-water emulsions and characterised using light scattering and microscopy and the wash water was further characterised separately.

#### 2.7. Protein content

The estimation of protein present in the SC supernatant and the wash water was performed using the BCA assay, which uses bicinchoninic acid (BCA) for the colourimetric quantification of total protein (Smith et al., 1985). After adding the working reagent, samples were incubated in a water bath at 37 °C for 30 min before measuring their absorbance at 562 nm. Results are presented as means and standard deviations, based on at least triplicate measurements conducted on three independent samples ( $n=3\times3$ ).

# 2.8. Sodium dodecyl sulphate polyacrylamide gel electrophoresis (SDS-PAGE)

The protein profile of SC supernatant and the wash water was analysed using sodium dodecyl sulfate-polyacrylamide gel electrophoresis (SDS-PAGE). A 1 mm thick Invitrogen NuPAGE (Thermo Scientific, Oxford, UK) gel consisting of 4–12 % Bis-Tris was used to load our samples in the wells. The gel was run in the Invitrogen mini gel tank (Thermo Scientific, Oxford, U.K.) setup at a constant voltage of 200 V for 35 min on a PowerEase 90 W power pack (Life Technologies, Thermo Scientific, Oxford, UK). A known protein standard (Novex Sharp Prestained Protein Standard, Invitrogen, Oxford, UK) of molecular weight 3.5–260 kDa was run alongside the samples. Finally, the gels were stained with Coomassie (SimplyBlue™ Sain, Invitrogen, Oxford, UK) for visualising the protein bands on the gel. Excess stain was washed off using distilled water and the protein electropherogram was imaged using a ChemiDoc XRS+ with Image Lab Software (Bio-Rad, Oxford, UK).

# 2.9. Emulsion stability

Droplet size distribution in the emulsions was monitored using a static light scattering instrument (Mastersizer 3000 series, Malvern, UK) with the obscuration set between 4 % and 6 %. To understand stability, the emulsions were monitored for droplet size measurement over a period of 30 days. Emulsions were also visually assessed in glass vials over this period. The mean droplet size distribution was reported and volume mean diameter (d [4,3]) was compared as a function of storage time at 22 °C. The refractive indices of the oil droplets and water were 1.46 and 1.33, respectively. Results are presented as means and standard deviations, based on at least triplicate measurements conducted on three independent samples ( $n=3\times3$ ). Coalescence rate in SC emulsion droplets (Sarkar et al., 2010; Walstra, 1987) containing 5 and 10 wt% proteins were calculated using eq. (1)

$$\frac{N_t}{N_0} = e^{-K_c t} \tag{1}$$

where,  $N_t$  is the number concentration of SC emulsion droplets at time t (days),  $N_0$  is the initial number concentration of freshly homogenized SC emulsion droplets (time zero) and Kc is the coalescence rate constant.

 $\begin{tabular}{ll} \textbf{Table 1}\\ Yield of biomass obtained using SC, NC$_1$ and NC$_2$ expressed as means and standard deviations of triplicate experiments. \end{tabular}$ 

Yield of biomass in g/L	SC	NC <sub>1</sub>	NC <sub>2</sub>
Dry weight	$5.8 \pm 1$	$5.6\pm1.1$	$6.7\pm0.2$
Wet weight	$20.6\pm1.1$	23.5	25.1

Using the transformation of the MasterSizer volume distribution data to the number distribution,  $(N_t/N_0)$  were plotted *versus* the time (days), with the slope denoting  $K_c$ .

#### 2.10. Confocal laser scanning microscopy (CLSM)

The microstructure of the biomass and the biomass-stabilised emulsions were characterised using an upright confocal laser scanning microscopy (CLSM) (Zeiss LSM 880, Carl Zeiss MicroImaging GmbH, Germany). Calcofluor White (1.0 % w/v in Milli-Q water, excitation 405 nm, emission 410–523 nm) was used to stain the chitin in the biomass. In case of the emulsions, Nile Red (0.1 % w/v in dimethyl sulphoxide, excitation 514 nm, emission 539–648 nm) was used to stain the oil droplets. Mixtures of biomass and dye (Calcofluor White), as well as the mixtures of emulsions with Calcofluor White and Nile Red, were vortexed for 10 s, equilibrated for 10 min, and then 30  $\mu$ L of the sample was placed onto a concave slide and the samples were observed using a 63× magnification oil immersion objective lens. *Z*-stack images of the emulsion were also captured, and a 3D micrograph was constructed using the Zen software (Carl Zeiss MicroImaging GmbH, Germany).

#### 2.11. Apparent viscosity

Apparent viscosity was measured using Anton Paar MCR 302 rheometer (Anton Paar, Germany) using RheoCompass software. 5–10 wt% dispersions of SC biomass was prepared in 20 mM phosphate buffer at pH 7.0 and placed between a 50 mm diameter cone-plate geometry (Anton Paar CP50–1). The gap was set to 0.1 mm and the sample was run at 25  $^{\circ}$ C measuring shear rates between  $1\,\mathrm{s}^{-1}$  to  $1000\,\mathrm{s}^{-1}$ . Deionised water and phosphate buffer without biomass were measured as control. The data was analysed using Origin Pro software. Viscosity for SC-

stabilised oil-in-water emulsions (5–10 wt% oil) were also measured containing 1 wt% biomass. Results are presented as means and standard deviations, based on at least triplicate measurements conducted on three independent samples ( $n=3\times3$ ).

#### 2.12. Statistical analysis

Unless stated otherwise, results are presented as means and standard deviations, based on at least three triplicate measurements conducted on three independent samples (n =  $3 \times 3$ ). Analysis of variance (ANOVA) with a Tukey *post hoc* test (p < 0.05) was performed to compare data sets, using Microsoft Excel (Version 2502) and OriginPro (version 2024b).

#### 3. Results and discussion

#### 3.1. Characteristics of yeast biomass

#### 3.1.1. Yield and microstructure

Briefly, yeasts were grown in YPD media where the yield of the biomass pellets obtained after batch fermentation is presented in Table 1. All strains had typical values reported for batch fermentation ranging from 20 to 40 g/L (Malairuang et al., 2020). NC2 strain produced the highest yield dry cell weight per litre, while SC and NC1 produced slightly lower yields (p > 0.05). To investigate differences in cell morphology, we characterised the microstructure of the biomass using microscopy across length scales, as shown in Figs. 2a-b. Morphologically, both SC and NC2 biomass exhibited pronounced spherical or slightly ovoid appearance as can be observed in the SEM images (Figs. 2a1-b1, a3-b3), while NC1 cells demonstrated elliptical shape with a 3:2 aspect ratio (Figs. 2a2-b2). In SEM images, it can also be noted that SC and NC2 cells show aggregation, whereas NC1 cells appeared to be well-separated (Figs. 2a1-a3). Notably, CLSM confirmed the presence of chitin-rich domains (green halo) in the cell wall fluoresced using Calcofluor White (Figs. 2b1-b3). NC2 exhibited higher levels and a rather homogeneous distribution of chitin throughout the cell body (Fig. 2b3), whilst the chitin distribution was less uniform in SC and NC1 with more preferential location at the edges of the cell wall shown by darker florescence (Figs. 2b1-b2).

Major cell axes were measured from both SEM and CLSM images (Fig. 2c). SC cells exhibited diameters of 3–5  $\mu$ m, NC<sub>2</sub> cells ranged from 3

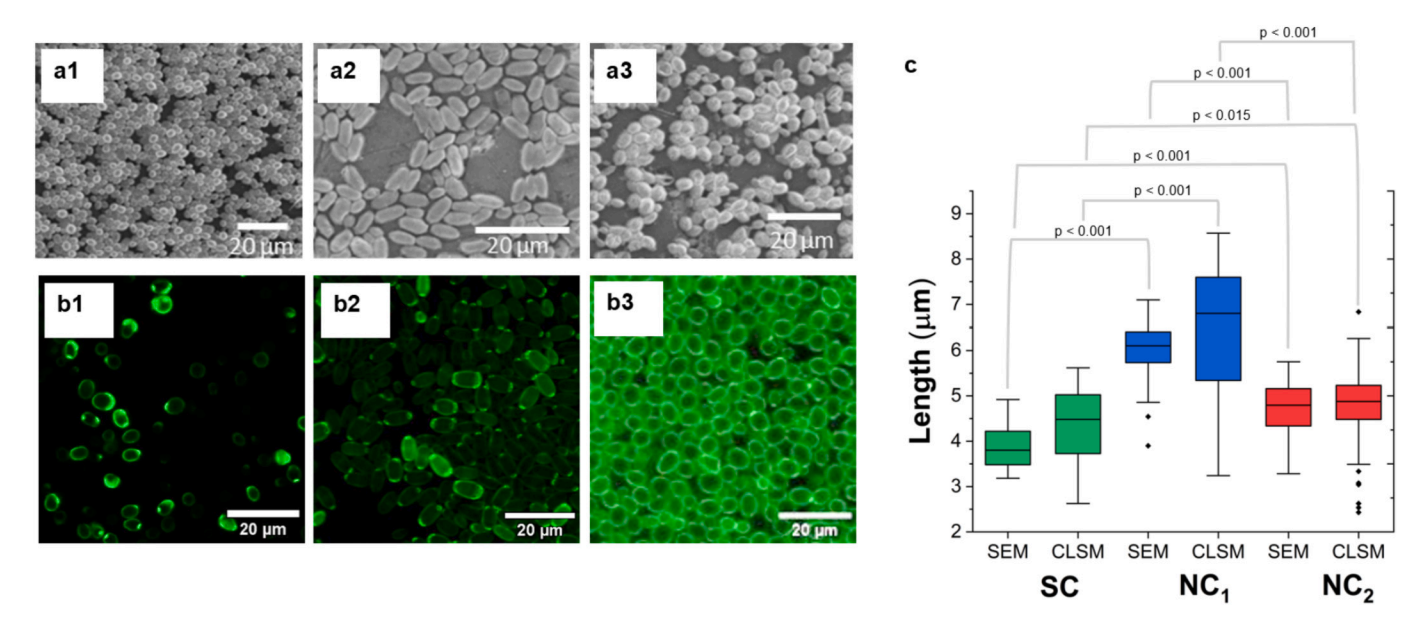


**Fig. 2.** Microstructure of the biomass analysed using (a) scanning electron microscopy (SEM), where 1, 2 and 3 are SC, NC<sub>1</sub> and NC<sub>2</sub>, respectively, (b) confocal laser scanning microscopy (CLSM), and (c) the length of the cells analysed using ImageJ using micrographs from (a) and (b), along with their *p* values.

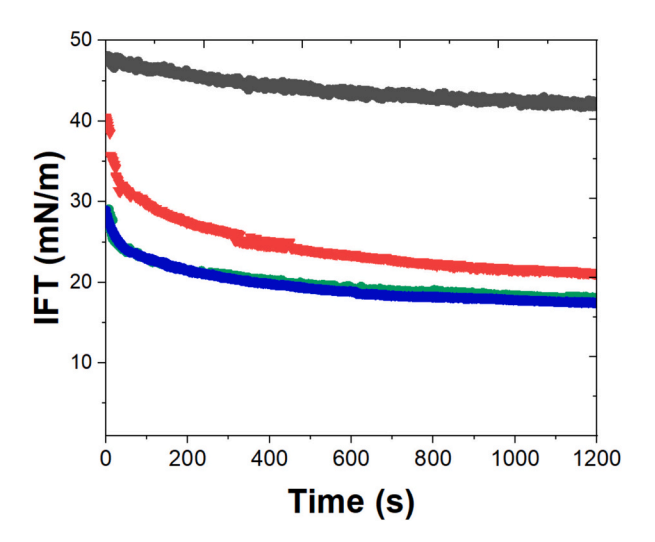


**Fig. 3.** Dynamic interfacial tension measurements (IFT) of n-tetradecane-water interface in presence of SC ( $\bullet$ ), NC<sub>1</sub> ( $\blacksquare$ ) and NC<sub>2</sub> ( $\blacktriangledown$ ). n-tetradecane-buffer interface (without biomass,  $\blacktriangle$ ) is shown as control. Data represent the average of three independent readings on triplicate samples ( $n=3\times3$ ). (For interpretation of the references to colour in this figure legend, the reader is referred to the web version of this article.)

to 6  $\mu$ m, and NC<sub>1</sub> cells were slightly larger, ranging from 5 to 8  $\mu$ m, which are in agreement with yeast biomass grown using similar batch fermentation techniques (Feldmann, 2012; Tofalo & Suzzi, 2016). There was no significant difference between the sizes of biomass measured using the SEM and CLSM images. But, there was a significant difference in the sizes of the three yeast biomass (p < 0.001) as shown in Fig. 2c.

#### 3.1.2. Interfacial tension

It is known that that microorganisms can decrease the interfacial tension by extracellular or cell-bound biosurfactants (Lang, 2002; Naughton et al., 2019). Hence, it was important to understand whether any difference exists in interfacial tension of the three yeast biomass tested in this study as a result of differing surface properties of these cells. Fig. 3 shows the dynamic interfacial tension between dispersions containing yeast biomass and n-tetradecane. In absence of any added biomass, the interfacial tension of *n*-tetradecane-buffer ranged from 48 to 43 mN/m, within previously reported values (Hsieh et al., 2021). Unsurprisingly, with the addition of yeast biomass, a significant drop in interfacial tension was observed (p < 0.01), which has been observed in previous study using yeast cells (Meirelles et al., 2018), yeast protein (Zheng et al., 2025) and yeast fibres (Kong et al., 2025). The timedependent adsorption behaviour of biomass was apparent across all samples with pronounced reduction in surface tension occurring within the first 60 s, despite slight differences in kinetics as well as final interfacial tension magnitudes recorded at 1200 s (p > 0.05). Particularly, with addition of SC or NC<sub>1</sub> biomass, the interfacial tension reduced to 17–19 mN/m within the first 10 min (Fig. 3). With NC<sub>2</sub> biomass, the reduction in interfacial tension was faster than the other two biomass samples but with a higher tension value of 21 mN/m (Fig. 3) however this was not significant (p > 0.05). Overall, this suggests that differences in emulsification ability (if any) might not be directly linked to how the biosurfactants at the cell's surface or the extracellular biosurfactant diffuse at the oil-water interface.

# 3.2. Characteristics of emulsions

# 3.2.1. Emulsions stabilised by three different yeast biomass

Oil-in-water emulsions were next prepared utilising the yeast biomasses. It is apparent from the large size of biomass (Fig. 2), the cells showed a high degree of sediment in the continuous phase which can be

observed by a thin bottom layer within the vials (Figs. 4a1-a3). Such sedimentation has been previously reported by other studies involving yeast-stabilised emulsions (Meirelles et al., 2018).

Focusing first on SC-stabilised emulsions, creaming of oil droplets was observed after 2 weeks (Fig. 4a1) due to density differences between the emulsion droplets and the continuous phase. No clear oil layer or phase separation was observed for SC-stabilised emulsions. Looking at the CLSM image of SC-stabilised emulsion (Fig. 4b1), it was clear that the sample had a distrbution of smaller-sized droplets ( $< 1 \mu m$ ) as well as larger-sized droplets (5–10  $\mu m$ ). It would be presumed that the biomass would form a monolayer as observed previously at the oil-water droplet interface for dehydrated yeast particles as described by Firoozmand & Rousseau (2016) with a complete coverage of droplet surface by the cells as demonstrated by Furtado et al. (2015) and Moreira et al. (2016). However, the CLSM observations in Fig. 4b1 and the 3D micrograph of the image in the inset of Fig. 4b1 revealed limited cells located at the droplet surface, with most SC cells being visible in the continuous phase, which suggests that the droplets might not have been stabilised by cells themselves. This is further discussed later. Figure 4c1 shows the droplet size distribution across a 4-week storage period, where SC-stabilised emulsions showed a bimodal distribution with the larger peak at about 20 µm. The smaller peak around 3 µm would likely be attributed to the SC cells in the biomass, which are around 3–5  $\mu m$  in length (Figs. 2a1-b1) but can also be due to smaller oil droplets in the emulsion as seen in Fig. 4b1. At day 28, we see the appearance of a third small peak at around 200 µm. This small peak might suggest flocculation/ some degree of droplet coalescence.

For NC<sub>1</sub>, the emulsions showed coalescence and macroscopic phase separation even within a day (Fig. 4a2). The cells did not anchor at the interface and preferred to be dispersed and sediment out in the continuous phase (Fig. 4b2) with clear droplet coalescence. NC<sub>1</sub>-stabilised emulsions showed a large peak at 20  $\mu$ m and a smaller second peak around 1  $\mu$ m (Fig. 4c2) similar to those of SC-stabilised droplets. The droplet size data did not show many changes for days 14 and 28. It is rather surprising that the coalescence was not reflected in the light scattering, which might occur owing to large coalesced oil droplets rising to the top and not taken into account in the cumulative analysis.

For NC2-stabilised emulsions, the samples showed rapid coalescence (Fig. 4a3) even within a day. Interestingly, we observe Nile Red fluorescence within NC2 cells as these are oleaginous species and able to store fat (Fig. 4b3). However, no emulsion droplet were visible, which suggest most droplets might have coalesced and somehow could not be imaged as they rose to the top of the coverslip. The NC<sub>2</sub>-stabilised emulsions demonstrated a broad peak around 0.1-10 µm, most likely representing the oleaginous yeasts as well as some oil droplets, which later increased to a large peak around 150 µm at days 14 and 28 (Fig. 4c3). This suggests that coalescence was most prominent in NC2stabilised emulsions among the three samples tested. Although all the samples showed reduction in interfacial tension (Fig. 3), this did not result in emulsion stability. This suggests that although the biomass irrespective of their types could migrate to the interface to reduce oilwater-tension, they were not forming a thick, viscoelastic interfacial film that is important to offer kinetic stability. Future studies should further investigate the interfacial shear rheology of the films created by the biomass. Overall despite instability, the SC-stabilised emulsion was the most stable among the three emulsions stabilised by biomass. Based on this, we proceeded with further assessment to understand the property of SC cells to stabilise 5-10 wt% oil-in-water emulsions. This was to understand the effect of lower oil loads on emulsion stability and, more importantly, to examine whether or not there would be complete coverage by SC cells at the droplet surface in lower droplet volume fractions.

#### 3.2.2. Characteristics of SC-stabilised emulsions with reduced oil load

Fig. 5a presents SC-stabilised emulsions with the lower oil load (5 and 10 wt%) at days 7 and 14. Similar to the 20 % O/W emulsions,

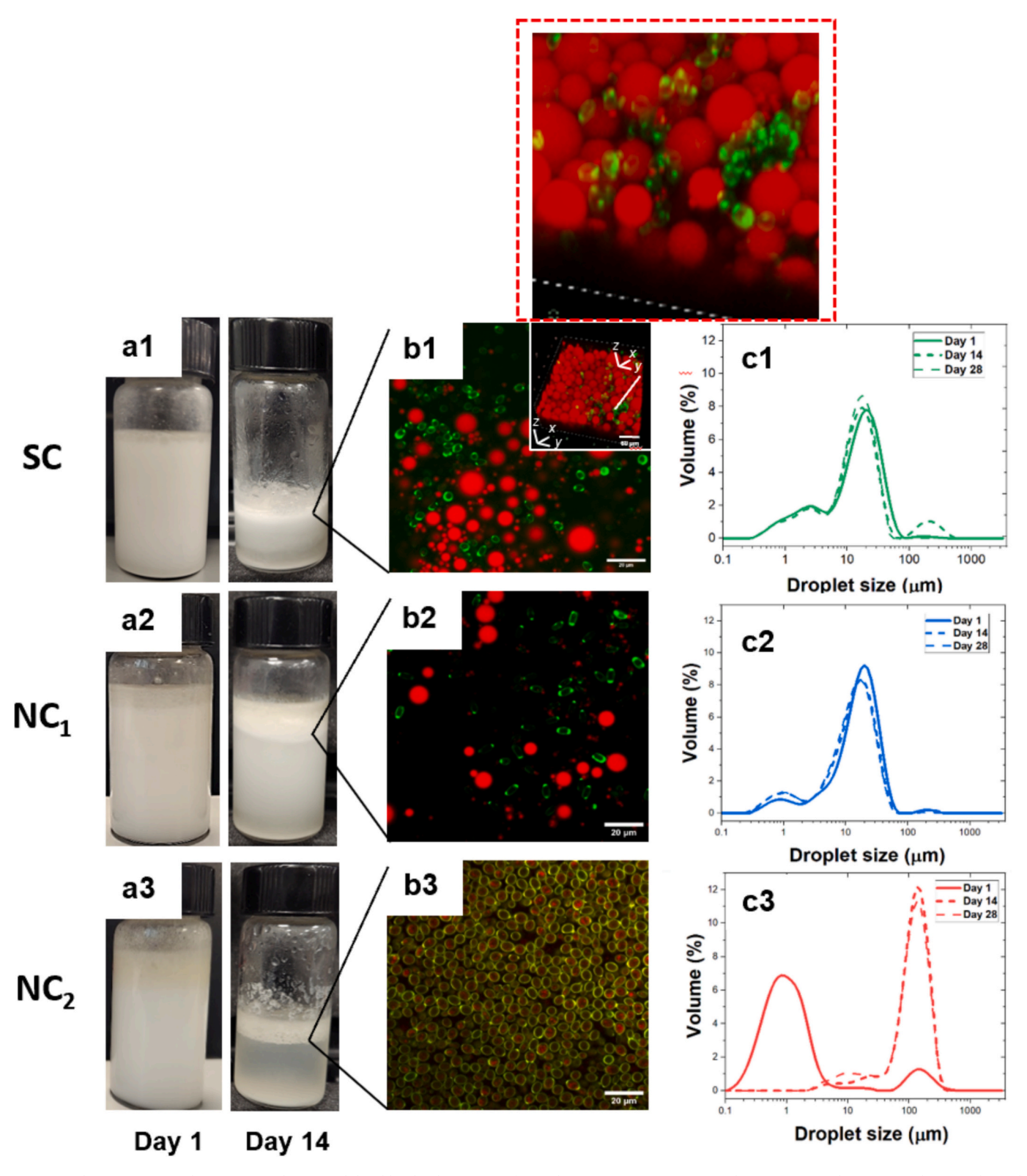


Fig. 4. Emulsions (20 wt% oil-in-water emulsions) stabilised by the three types of yeast biomass [SC (1), NC<sub>1</sub> (2) and NC<sub>2</sub> (3)]. Visual images (a) showing physical stability, (b) confocal micrographs of emulsion droplets taken on Day 14, where b1 also shows a 3D plot of SC as a small inset with a zoomed CLSM micrograph in red dotted line. Oil droplets stained in red using Nile Red, excited at 514 nm, and SC biomass in green stained using Calcofluor White, excited at 405 nm, and (c) mean droplet size distribution for the emulsions on day 1, 14 and 28, respectively. The scale bars in CLSM images represent 20  $\mu$ m. Data in (c) represent the average of three independent readings on triplicate samples (n = 3 × 3). (For interpretation of the references to colour in this figure legend, the reader is referred to the web version of this article.)

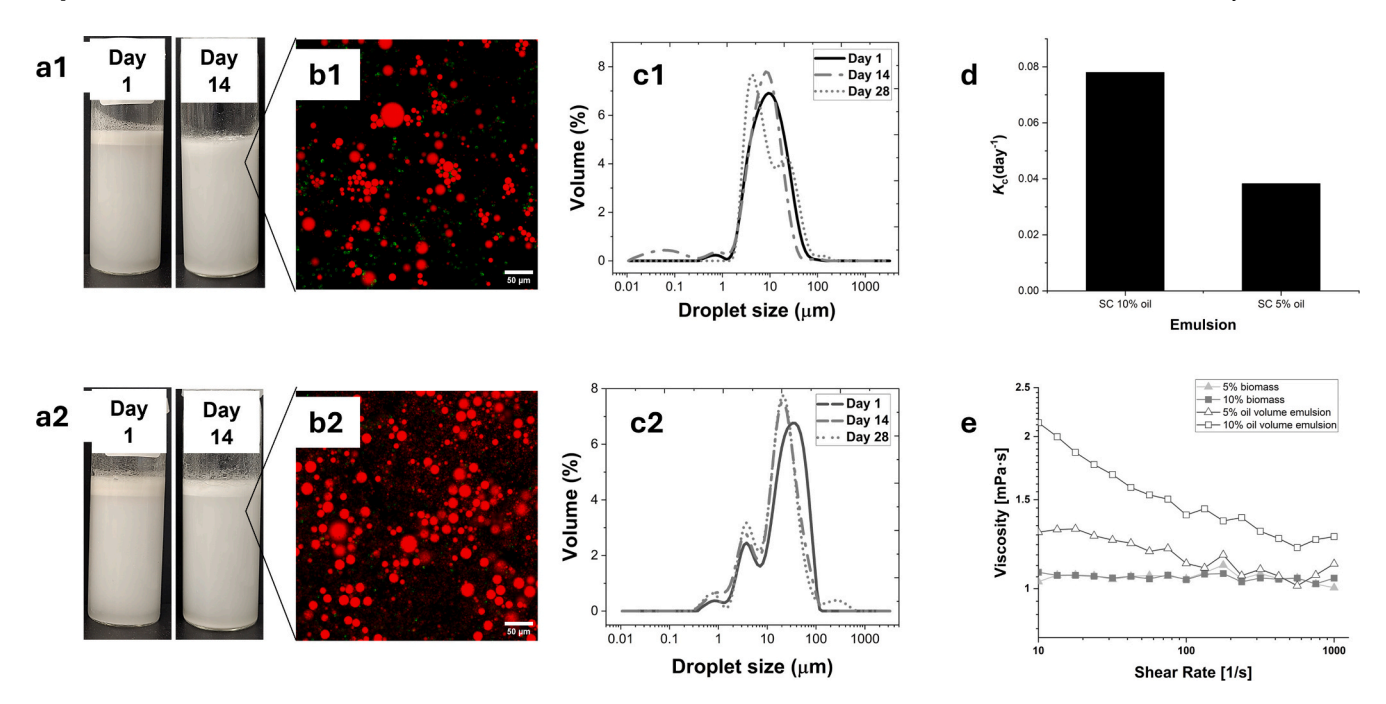


Fig. 5. Emulsions containing lower oil concentrations (of 5 to 10 wt% oil) stabilised by SC biomass. Visual images of SC biomass containing (a1) 5 wt% oil and (a2) 10 wt% oil showing physical stability. (b) Confocal micrographs of emulsion droplets taken on Day 14. Oil droplets stained in red using Nile Red, excited at 514 nm, and SC biomass in green stained using Calcofluor White, excited at 405 nm, and (c) mean droplet size distribution for the emulsions on day 1, 14 and 28, respectively. The scale bars in CLSM images represent 50  $\mu$ m. (d) The coalescence rate for SC-stabilised emulsions containing 10 wt% and 5 wt% oil. (e) Apparent viscosity of SC biomass at 5 % and 10 % volumes (closed symbols) and SC-stabilised emulsions with 5 wt% and 10 wt% oil concentrations (open symbols). Data in (c) and (e) represent the average of three independent readings on triplicate samples (n = 3  $\times$  3).

sedimentation of biomass particles was observed at the bottom of the vials, along with creaming at the top. From the CLSM emulsion micrographs (Fig. 5b), the proportion of smaller sized droplets were apparent in 5 wt% as compared to 10 wt% (Figs. 5b1-b2). However, unlike what has been previously reported for rehydrated yeast particles covering droplet surface (Firoozmand & Rousseau, 2016; Furtado et al., 2015; Meirelles et al., 2018; Moreira et al., 2016), even at lower oil loads, no biomass could be located at the droplet surfaces.

From Fig. 5c1, SC-stabilised emulsion with 5 wt% oil demonstrated a smaller droplet size ranging from 2 to 70  $\mu m,$  while those with 10 wt% oil (Fig. 5c2) had droplets in the  $0.3~\mu m$  to  $600~\mu m$  range over the one month period. Also, the emulsion with 5 wt% oil concentrations exhibit a monomodal size distribution as compared to the emulsions with 10 wt % oil concentration which had a bimodal droplet size distribution. The emulsions with 10 wt% oil load (Fig. 5c2) also showed a third peak after 4 weeks indicating droplet coalescence as was also observed in the system containing 20 wt% oil (Fig. 4c1). Overall, SC-stabilised emulsions containing 5 wt% oil was kinetically more stable than those containing 10 or 20 wt% oil concentrations, which was clear from light scattering data as well as microscopy data (Figs. 4a1-c1 and 5a1-c2). Additionally, comparing the coalescence rate  $(K_c, day^{-1})$  for the SCstabilised emulsions containing 5 wt% and 10 wt% oil (Fig. 5d), it was clear that coalescence rate was reduced by half when the oil load was decreased. This is expected as the same quantity of yeast cells are now present to stabilise reduced quantity of surface.

The viscosity of SC biomass at 5 wt% and 10 wt% concentrations in phosphate buffer exhibits a Newtonian behaviour with viscosity resembling buffer as indicated in Fig. 5e, which might suggests that cells are settling out and any viscosity measurements should be taken with caution. From Fig. 5e, we can observe that SC-stabilised emulsions containing 5 wt% and 10 wt% oil show a reduction in viscosity with increasing shear rates indicating typical non-Newtonian behaviour associated with flocculating emulsions where blocks break as a function of shear forces.

There have been studies showing the stability of particle-stabilised

emulsions even with poor droplet coverage by the particles (Destribats et al., 2014). However, irrespective of droplet volume fraction, limited coverage of droplets surface was observed by SC biomass (Figs. 5b1, 5b2). Therefore, we hypothesize that unlike the previously reported Pickering stabilisation mechanism (Firoozmand & Rousseau (2016); Furtado et al., 2015; Meirelles et al., 2018; Moreira et al., 2016), oil droplets are being stabilised by a biosurfactant in this study, other than the biomass themselves acting purely as Pickering stabilisers. We suggest that either the surface proteins (e.g. mannoprotein) or other biosurfactants released from the cells during homogenisation or potentially surface active compounds from the YPD media are contributing to stabilising the oil droplets. While high-pressure homogenisation techniques are often employed for cell lysis, the pressures typically used often fall within the range of 100 to 600 MPa (Escott et al., 2025) and are significantly higher than what we applied in our emulsion formation. Our emulsions are relatively low in viscosity, consisting of oil volumes of 20 % or less, which may further diminish the likelihood of shear-induced cell breakage (Clarke et al., 2010). Furthermore, observations using CLSM revealed intact cells (Figs. 4b and 5b), which did not exhibit clear signs of cell breakage. This suggests that the emulsification process did not significantly compromise cell integrity and surface proteins such as mannoproteins were potentially stabilising the droplets.

Mannoproteins are reported as good stabilisers of emulsions and studies with extracted mannoproteins from *Saccharomyces* species have been described in literature (Cameron et al., 1988; Li & Karboune, 2019; Meirelles et al., 2018; Qiao et al., 2022; Reis et al., 2023; Torabizadeh et al., 1996). Hence, mannoproteins leaching out of the cells and stabilising the SC emulsion droplets *via* a pure molecularly-adsorbed process seems like the mechanism, which also is in line with the reduction of interfacial tension (Fig. 3).

# 3.3. Effect of washing on emulsion stability

To further validate the role of molecularly-adsorbed biosurfactant in stabilising the SC emulsion droplets, SC biomass was washed to remove

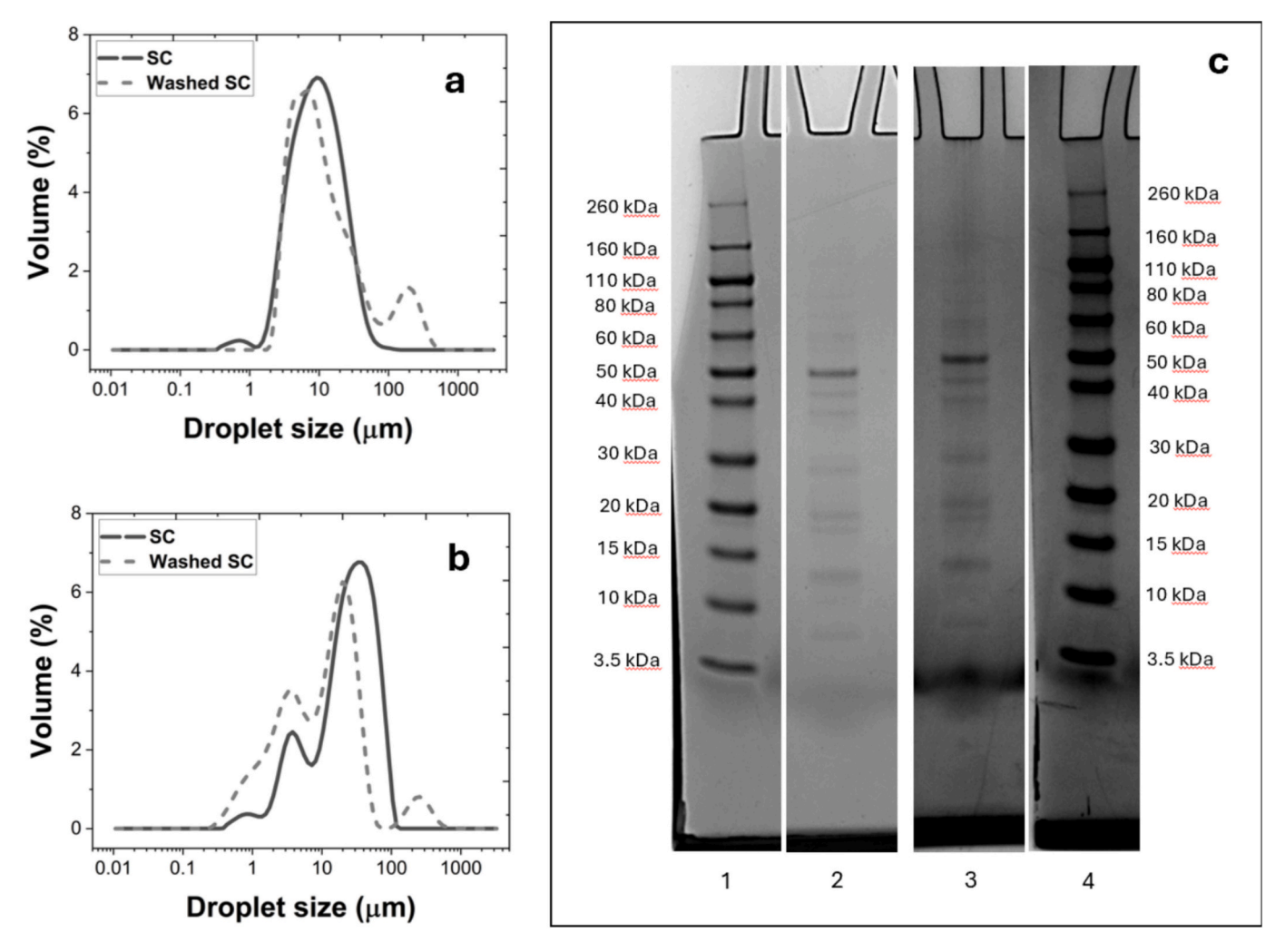


Fig. 6. Mean droplet size distribution of emulsions stabilised by SC biomass (washed or unwashed) containing (a) 5 wt% oil, (b) and 10 wt% oil, respectively, on day 1. Data represent the average of three independent readings on triplicate samples ( $n = 3 \times 3$ ). (c) Sodium dodecyl sulphate polyacrylamide gel electrophoresis (SDS-PAGE), where lane 1 and lane 4 are molecular weight protein ladder, while lane 2 shows the run profile of SC supernatant and lane 3 shows the SC washed water.

any loosely-bound biosurfactants as described in **Figure1**. Droplet size distribution of 5 wt% and 10 wt% oil containing SC emulsions are shown in Fig. 6. In Fig. 6a, we observe that the droplet size of the emulsion with washed biomass shows a bimodal distribution with the largest peak between 2  $\mu m$  and 80  $\mu m$ . More importantly, there is a smaller peak between 80  $\mu m$  and 500  $\mu m$  in the system stabilised by washed biomass, which is absent in the non-washed ones, indicating the importance of water-soluble biosurfactants in the stabilisation mechanism. The mean droplet sizes (d [4,3] values) of washed SC-stabilised emulsions were larger than those stabilised by the unwashed counterparts at 5 wt% oil concentration (p < 0.001).

Similarly, Fig. 6b shows the comparison of droplet size distribution between washed and unwashed SC biomass-stabilised emulsions with  $10~\rm wt\%$  oil concentration. Again, it is clear that the washed SC-stabilised emulsion shows a trimodal distribution patter with a smaller peak at  $250~\mu m$  highlighting droplet coalescence. This suggests the importance of water-soluble bio-surfactants contributing to the stabilisation mechanism. We then questioned whether the washed water from the cells contained any protein and then characterised the protein composition and quantity to confirm their role in emulsion stabilisation.

The protein content of the SC supernatant and wash water was estimated using the BCA protein assay. The protein content of the supernatant was 4618  $\mu$ g/mg, while that of the wash water was 534  $\mu$ g/mg highlighting that there was still 88 % of total protein present with the cells that were potentially contributing to the emulsion stabilisation.

The protein composition of the SC supernatant and wash water are shown in Fig. 6c. SC supernatant and washing water showed similar molecular weight distribution and band patterns. The visible bands ranged in molecular weights from 7 to 80 kDa, with faint bands between 80 and 160 kDa, these are most likely mannoproteins. Mannoprotein can range in molecular weights of 5 to 800 kDa (Narsipur et al., 2024; Wan et al., 2021). Several studies have tried to quantify different protein fractions of mannoprotein using chromatographic, SDS-PAGE and mass spectrometric techniques. Spontón et al. (2015) identified purified mannoprotein extracts from SC in the rage of 6.5–30 kDa. The SDS-PAGE profile of mannoproteins from a previous study (Silva Araújo et al., 2014) showed proteins of 58 and 64 kDa. (Li et al. (2020)) used various extraction methods to extract mannoproteins from SC cell walls. They observed bands in a wide range of molecular weights between 2 and 100 kDa.

Besides mannoproteins, it is noteworthy that our yeast was cultured in the lab in a batch fermentation from frozen cell stocks. They were grown in complex culture media *i.e.* YPD. This media contains all the amino acids needed for the growth of the cells. These protein components from the media might have surface activity and aid in stabilising the emulsions. However, washing the cells with water removes some of these water-soluble proteinaceous elements carried over from the media (Meirelles et al., 2018). In addition to mannoproteins and YPD media-asociated remnants, cytoplasmic proteins from autolysed yeast cells produced during homogenisation also cannot be ignored.

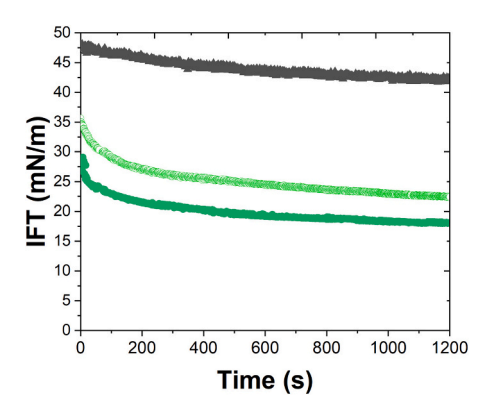


**Fig. 7.** Dynamic interfacial tension measurements (IFT) of n-tetradecane-water interface in presence of SC ( $\bigcirc$ , closed symbol), and washed SC ( $\bigcirc$ , open symbol). n-tetradecane-buffer interface (without biomass,  $\blacktriangle$ ) is shown as control. Data represent the average of three independent readings on triplicate samples ( $n=3\times3$ ). (For interpretation of the references to colour in this figure legend, the reader is referred to the web version of this article.)

To finally confirm this from an interfacial perspective, it was clear that post washing the tension at *n*-tetradecane-buffer interface increases to 23 mN/M after 20 min (Fig. 7). This suggests that the washing step has removed not only the proteins (Fig. 6), but more importantly interfacially-active proteins that were present at the surface of the biomass. This suggests that the yeast biomass stabilisation in this particular study was largely linked to molecularly-adsorbed interfacial stabilisation rather than a Pickering-type stabilisation (Firoozmand & Rousseau (2016); Furtado et al., 2015; Meirelles et al., 2018; Moreira et al., 2016). A key limitation of this study was that the biomass often tends to sediment, which also influences the emulsion stabilisation and interfacial characterisation such as interfacial tension measurement and bulk viscosity. This suggests further characterisation techniques need to be developed to pinpoint stabilisation mechanism when dealing with these micron-sized large particles.

#### 4. Conclusions

In this study, three different strains of food-grade yeast were cultured using batch fermentation. Overall, S. cerevisiae biomass offered better emulsion stabilising properties than NC<sub>1</sub> and NC<sub>2</sub> biomass, with no coalescence or phase separation observed for 4 weeks in the former. However, emulsions prepared using washed S. cerevisiae biomass were found to be less stable than the unwashed ones largely associated with depletion of interfacially-active proteins. We hypothesize that surface proteins such as mannoproteins or proteins that might have been secreted from the biomass during homogenisation process are essential in stabilising yeast biomass-based emulsions via a molecularly stabilisation mechanism. Overall, this suggests that yeast cell-stabilised emulsions might not be stabilised by a pure Pickering mechanism as often reported in literature, particular for rehydrated yeast powders. Ongoing studies are focusing on isolating which specific mannoproteins at the surface or proteins leached out from the yeasts during homogenisation are contributing to this emulsion stabilisation effect. Such knowledge is crucial before yeast biomass can be used for emulsion stabilisation for preparation of alternative-protein rich foods without additional extraction processes.

#### CRediT authorship contribution statement

**Sowmya Narsipur:** Writing – review & editing, Writing – original draft, Visualization, Validation, Methodology, Investigation, Formal analysis, Data curation. **Qifei He:** Formal analysis. **Ben Kew:** Writing – review & editing, Visualization, Methodology, Data curation. **Célia Ferreira:** Writing – review & editing, Supervision, Methodology.

**Anwesha Sarkar:** Writing – review & editing, Supervision, Methodology, Funding acquisition, Conceptualization.

#### **Declaration of competing interest**

The authors declare that they have no known competing financial interests or personal relationships that could have appeared to influence the work reported in this paper.

#### Acknowledgements

Authors gratefully acknowledge the Engineering and Physical Sciences Research Council (EPSRC) funded Centre for Doctoral Training in Molecules to Product, Grant Ref. No. EP/S022473/1 for financial support. Author (AS) acknowledges UK National Alternative Proteins Innovation Centre (NAPIC), which is an Innovation and Knowledge Centre funded by the Biotechnology and Biological Sciences Research Council (BBSRC) and Innovate UK (Grant Ref: BB/Z516119/1). The authors would like to gratefully acknowledge the technical support in Confocal Laser Scanning Microscopy Facility at the Bio-imaging and Flow Cytometry facility in the Faculty of Biological Sciences. Graphical abstract was created in BioRender. Kew, B. (2025) https://BioRender.com/m6mpgzj. Figure 1 was created in BioRender. Narsipur, S. (2025) https://BioRender.com/pwpzoak.

# Data availability

Data will be made available on request.

#### References

Akgonullu, D. Z., O'Hagan, N. M., Murray, B. S., Connell, S. D., Fang, Y., Linter, B. R., & Sarkar, A. (2024). Bulk and interfacial behavior of potato protein-based microgels. Langmuir, 40(41), 21341–21351. https://doi.org/10.1021/acs.langmuir.4c01785

Berry, J. D., Neeson, M. J., Dagastine, R. R., Chan, D. Y. C., & Tabor, R. F. (2015). Measurement of surface and interfacial tension using pendant drop tensiometry. *Journal of Colloid and Interface Science*, 454, 226–237. https://doi.org/10.1016/j.jcis.2015.05.012

Cameron, D. R., Cooper, D. G., & Neufeld, R. J. (1988). The mannoprotein of Saccharomyces cerevisiae is an effective bioemulsifier. Applied and Environmental Microbiology, 54(6), 1420–1425. https://doi.org/10.1128/aem.54.6.1420-1425\_1988

Clarke, A., Prescott, T., Khan, A., & Olabi, A. G. (2010). Causes of breakage and disruption in a homogeniser. Applied Energy, 87(12), 3680–3690. https://doi.org/ 10.1016/j.apenergy.2010.05.007

Destribats, M., Rouvet, M., Gehin-Delval, C., Schmitt, C., & Binks, B. P. (2014). Emulsions stabilised by whey protein microgel particles: Towards food-grade Pickering emulsions. Soft Matter, 10(36), 6941–6954. https://doi.org/10.1039/C4SM00179F

Dorobantu, L. S., Yeung, A. K. C., Foght, J. M., & Gray, M. R. (2004). Stabilization of oil-water emulsions by hydrophobic bacteria. *Applied and Environmental Microbiology, 70* (10), 6333–6336. https://doi.org/10.1128/AEM.70.10.6333-6336.2004

Escott, C., Vaquero, C., Loira, I., Tat, L., López, C., González, C., & Morata, A. (2025). Influence of ultra-high pressure homogenization (UHPH) in the fermentability of Tempranillo musts by Saccharomyces and non-Saccharomyces. *Lwt*, 223, Article 117746. https://doi.org/10.1016/i.lwt.2025.117746

Feldmann, H. (2012). Yeast cell architecture and functions. In Yeast (pp. 5–24). Wiley-Blackwell.

Firoozmand, H., & Rousseau, D. (2016). Microbial cells as colloidal particles: Pickering oil-in-water emulsions stabilized by bacteria and yeast. *Food Research International*, 81, 66–73. https://doi.org/10.1016/j.foodres.2015.10.018

Furtado, G. F., Picone, C. S. F., Cuellar, M. C., & Cunha, R. L. (2015). Breaking oil-in-water emulsions stabilized by yeast. *Colloids and Surfaces B: Biointerfaces*, 128, 568–576. https://doi.org/10.1016/j.colsurfb.2015.03.010

Held, P. G. (2010). Monitoring growth of beer brewing strains of Saccharomyces Cerevisiae using the Agilent BioTek synergy H1 multimode reader to provide high quality kinetic data for yeast growth application.

Hsieh, T.-L., Law, S., Garoff, S., & Tilton, R. D. (2021). Ph-dependent interfacial tension and dilatational modulus synergism of oil-soluble fatty acid and water-soluble cationic surfactants at the oil/water interface. *Langmuir*, 37(39), 11573–11581. https://doi.org/10.1021/acs.langmuir.1c01889

Inaba, H., & Sato, K. (1996). A measurement of interfacial tension between tetradecane and ethylene glycol water solution by means of the pendant drop method. Fluid Phase Equilibria, 125(1), 159–168. https://doi.org/10.1016/S0378-3812(96)03085-3

Jiang, X., Yucel Falco, C., Dalby, K. N., Siegumfeldt, H., Arneborg, N., & Risbo, J. (2019). Surface engineered bacteria as Pickering stabilizers for foams and emulsions. Food Hydrocolloids, 89, 224–233. https://doi.org/10.1016/j.foodhyd.2018.10.044

- Kong, Y., Chen, J., Hong, Z., Guo, R., & Huang, Q. (2025). Insights into the Pickering emulsions stabilized by yeast dietary fiber: Interfacial adsorption kinetics, rheological characteristics, and stabilization mechanisms. Food Chemistry, 464, Article 141924. https://doi.org/10.1016/j.foodchem.2024.141924
- Lang, S. (2002). Biological amphiphiles (microbial biosurfactants). Current Opinion in Colloid & Interface Science, 7(1), 12–20. https://doi.org/10.1016/S1359-0294(02) 00007-9
- Li, J., & Karboune, S. (2019). Characterization of the composition and the technofunctional properties of mannoproteins from Saccharomyces cerevisiae yeast cell walls. Food Chemistry, 297, Article 124867. https://doi.org/10.1016/j. foodchem.2019.05.141
- Li, J., Karboune, S., & Asehraou, A. (2020). Mannoproteins from inactivated whole cells of baker's and brewer's yeasts as functional food ingredients: Isolation and optimization. *Journal of Food Science*, 85(5), 1438–1449. https://doi.org/10.1111/ 1750-3841.15054
- Lipke, P. N., & Ovalle, R. (1998). Cell wall architecture in yeast: New structure and new challenges. *Journal of Bacteriology*, 180(15), 3735–3740. https://doi.org/10.1128/ jb.180.15.3735-3740.1998
- Ma, K. K., Greis, M., Lu, J., Nolden, A. A., McClements, D. J., & Kinchla, A. J. (2022). Functional performance of plant proteins. Foods, 11(4). https://doi.org/10.3390/foods11040594
- Malairuang, K., Krajang, M., Sukna, J., Rattanapradit, K., & Chamsart, S. (2020). High cell density cultivation of Saccharomyces cerevisiae with intensive multiple sequential batches together with a novel technique of fed-batch at cell level (FBC). *Processes*, 8(10), 1321. https://www.mdpi.com/2227-9717/8/10/1321.
- Martin, G. J. O., & Chan, S. (2024). Future production of yeast biomass for sustainable proteins: A critical review. Sustainable Food Technology, 2(6), 1592–1609. https://doi.org/10.1039/D4FB00164H
- McLauchlan, J., Tyler, A. I. I., Chakrabarti, B., Orfila, C., & Sarkar, A. (2024). Oat protein: Review of structure-function synergies with other plant proteins. *Food Hydrocolloids*, 154, Article 110139. https://doi.org/10.1016/j.foodhyd.2024.110139
- Meirelles, A. A. D., da Cunha, R. L., & Gombert, A. K. (2018). The role of Saccharomyces cerevisiae in stabilizing emulsions of hexadecane in aqueous media. *Applied Microbiology and Biotechnology*, 102(7), 3411–3424. https://doi.org/10.1007/ s00253-017-8725-3
- Moreira, T. C. P., da Silva, V. M., Gombert, A. K., & da Cunha, R. L. (2016). Stabilization mechanisms of oil-in-water emulsions by Saccharomyces cerevisiae. *Colloids and Surfaces B: Biointerfaces*, 143, 399–405. https://doi.org/10.1016/j. colsurfb.2016.03.043
- Mortensen, A., Aguilar, F., Crebelli, R., Di Domenico, A., Dusemund, B., Frutos, M. J., & Lambré, C. (2017). Re-evaluation of sorbitan monostearate (E 491), sorbitan tristearate (E 492), sorbitan monolaurate (E 493), sorbitan monopalmitate (E 495) when used as food additives. EFSA Journal, 15(5), Article e04788. https://doi.org/10.2903/j.efsa.2017.4788
- Narsipur, S., Kew, B., Ferreira, C., El-Gendy, R., & Sarkar, A. (2024). Emulsion stabilised by yeast proteins and biomass: A mini review. *Current Opinion in Food Science*, 57, Article 101167. https://doi.org/10.1016/j.cofs.2024.101167
- Naughton, P. J., Marchant, R., Naughton, V., & Banat, I. M. (2019). Microbial biosurfactants: Current trends and applications in agricultural and biomedical industries. *Journal of Applied Microbiology*, 127(1), 12–28. https://doi.org/10.1111/jam\_14243
- Nerome, S., Onishi, M., Saito, D., Mizobuchi, A., Ando, T., Daira, Y., & Azuma, M. (2020). Cell surface changes that advance the application of using yeast as a food emulsifier. Food Chemistry, 315, Article 126264. https://doi.org/10.1016/j. foodchem.2020.126264.
- Nerome, S., Tsuzuki, M., Nizuka, M., Takata, M., Ojima, Y., & Azuma, M. (2023). Identification of emulsification proteins released from the cells by inhibiting the synthesis of GPI-anchor or β-1,3-glucan in Candida albicans. *Journal of Microbiological Methods*, 209, Article 106728. https://doi.org/10.1016/j.mimet.2023.106728
- Neto, R. O., & Silva, E. K. (2026). Yeast-derived hydrocolloids: Extraction strategies, functional properties and food applications of mannoproteins and β-glucans A review. Food Hydrocolloids, 171, Article 111764. https://doi.org/10.1016/j.foodbyd/2025.111764
- Okeudo-Cogan, M. C., Murray, B. S., Ettelaie, R., Connell, S. D., Peckham, M., Hughes, R. E., & Sarkar, A. (2025). Unravelling protein–fungal hyphae interactions at the nanoscale. ACS Applied Materials & Interfaces. https://doi.org/10.1021/ acsami.5c01064
- Okeudo-Cogan, M. C., Murray, B. S., Ettelaie, R., Connell, S. D., Radford, S. J., Micklethwaite, S., & Sarkar, A. (2023). Understanding the microstructure of a functional meat analogue: Demystifying interactions between fungal hyphae and egg

- white protein. Food Hydrocolloids, 140, Article 108606. https://doi.org/10.1016/j. foodhyd.2023.108606
- Okeudo-Cogan, M. C., Yang, S., Murray, B. S., Ettelaie, R., Connell, S. D., Radford, S., & Sarkar, A. (2024). Multivalent cations modulating microstructure and interactions of potato protein and fungal hyphae in a functional meat analogue. *Food Hydrocolloids*, 149, Article 109569. https://doi.org/10.1016/j.foodhyd.2023.109569
- Onishi, M., Ueda, M., Saito, D., Takata, M., Ojima, Y., & Azuma, M. (2021). Identification of yeast-derived emulsification proteins through analyses of proteins distributed into the emulsified phase. Food Hydrocolloids, 112, Article 106321. https://doi.org/ 10.1016/j.foodhyd.2020.106321
- Parapouli, M., Vasileiadis, A., Afendra, A. S., & Hatziloukas, E. (2020). Saccharomyces cerevisiae and its industrial applications. AIMS Microbiology, 6(1), 1–31. https://doi. org/10.3934/microbiol.2020001
- Pérez-Torrado, R., Gamero, E., Gómez-Pastor, R., Garre, E., Aranda, A., & Matallana, E. (2015). Yeast biomass, an optimised product with myriad applications in the food industry. *Trends in Food Science & Technology*, 46(2, Part A), 167–175. https://doi.org/10.1016/j.itifs.2015.10.008
- Qiao, Y., Xia, C., Liu, L., Tang, L., Wang, J., Xu, C., & Cui, Z. (2022). Structural characterization and emulsifier property of yeast mannoprotein enzymatically prepared with a β-1,6-glucanase. *Lwt*, *168*, Article 113898. https://doi.org/10.1016/i.lwt.2022.113898
- Reis, S. F., Fernandes, P. A. R., Martins, V. J., Gonçalves, S., Ferreira, L. P., Gaspar, V. M., & Coelho, E. (2023). Brewer's spent yeast Cell Wall polysaccharides as vegan and clean label additives for mayonnaise formulation. *Molecules*, 28(8). https://doi.org/ 10.3390/molecules28083540
- Saito, D., Nerome, S., Tachiwana, M., Ojima, Y., & Azuma, M. (2025). Yeast cell wall-derived proteins: Identification and characterization as food emulsifiers. Food Hydrocolloids, 160, Article 110746. https://doi.org/10.1016/j.foodhyd.2024.110746
- Sarkar, A., & Dickinson, E. (2020). Sustainable food-grade Pickering emulsions stabilized by plant-based particles. Current Opinion in Colloid & Interface Science, 49, 69–81. https://doi.org/10.1016/j.cocis.2020.04.004
- Sarkar, A., Horne, D. S., & Singh, H. (2010). Pancreatin-induced coalescence of oil-in-water emulsions in an in vitro duodenal model. *International Dairy Journal*, 20(9), 589–597. https://doi.org/10.1016/j.idairyj.2009.12.007
- Silva Araújo, V. B. D., Melo, A. N. F. D., Costa, A. G., Castro-Gomez, R. H., Madruga, M. S., Souza, E. L. D., & Magnani, M. (2014). Followed extraction of β-glucan and mannoprotein from spent brewer's yeast (Saccharomyces uvarum) and application of the obtained mannoprotein as a stabilizer in mayonnaise. *Innovative Food Science & Emerging Technologies*, 23, 164–170. https://doi.org/10.1016/j. ifset 2013.12.013
- Smith, P. K., Krohn, R. I., Hermanson, G. T., Mallia, A. K., Gartner, F. H., Provenzano, M. D., & Klenk, D. C. (1985). Measurement of protein using bicinchoninic acid. *Analytical Biochemistry*, 150(1), 76–85. https://doi.org/10.1016/ 0003-2697(85)90442-7
- Spontón, P. G., Spinelli, R., Drago, S. R., Tonarelli, G. G., & Simonetta, A. C. (2015). Acetylcholinesterase-inhibitor hydrolysates obtained from 'in vitro' enzymatic hydrolysis of mannoproteins extracted from different strains of yeasts. *International Journal of Food Science and Technology*, 51(2), 300–308. https://doi.org/10.1111/ iifs 12940
- Tofalo, R., & Suzzi, G. (2016). Yeasts. In B. Caballero, P. M. Finglas, & F. Toldrá (Eds.), Encyclopedia of food and health (pp. 593–599). Oxford: Academic Press.
- Torabizadeh, H., Shojaosadati, S. A., & Tehrani, H. A. (1996). Preparation and characterisation of bioemulsifier fromSaccharomyces cerevisiaeand its application in food products. LWT - Food Science and Technology, 29(8), 734–737. https://doi.org/ 10.1006/fstl.1996.0114
- Walstra, P. (1987). Physical principles of emulsion science. In J. M. V. Blanshard, & P. Lillford (Eds.), Food structure and behaviour (pp. 87–106). London, UK: Academic Press.
- Wan, M., Wang, M., Zhao, Y., Deng, H., Tan, C., Lin, S., & Meng, X. (2021). Extraction of mannoprotein from Saccharomyces cerevisiae and analysis of its chemical composition and molecular structure. *International Journal of Biological Macromolecules*, 193, 2252–2259. https://doi.org/10.1016/j.ijbiomac.2021.11.057
- Wani, A. K., Rahayu, F., Yustina, I., Fatah, G. S. A., Kariada, I. K., Antarlina, S. S., & Pamungkas, D. (2023). Contribution of yeast and its biomass for the preparation of industrially essential materials: A boon to circular economy. *Bioresource Technology Reports*, 23, Article 101508. https://doi.org/10.1016/j.biteb.2023.101508
- Zheng, X., Cheng, T., Liu, S., Tian, Y., Liu, J., Wang, Z., & Guo, Z. (2025). Ultrasonic combined pH shifting strategy for improving the stability of emulsion stabilized by yeast proteins: Focused on solubility, protein structure, interface properties. International Journal of Biological Macromolecules, 293, Article 139396. https://doi.org/10.1016/j.ijbiomac.2024.139396